



Bulk and Interfacial Effects in Co–Cr₂O₃ Nanocomposites

M. Farooq Nasir^{1,*}, Huey Hoon Hng², K. O'Grady³, and Sadia Manzoor¹

¹Department of Physics, COMSATS Institute of Information Technology, Park Road, Islamabad 44000, Pakistan

²School of Materials Science and Engineering, Nanyang Technological University, Singapore 639798

³Department of Physics, University of York, Heslington, York YO10 5DD, UK

The exchange bias field has been measured in a set of Co–Cr₂O₃ nanocomposites in order to distinguish between the bulk and interfacial contributions to H_{ex} . The studies were carried out on a set of samples prepared by the sol gel technique in which the Co concentration was varied between 30 and 80 wt%. The particle sizes in all samples were carefully controlled so as to enable a comparison of their magnetic properties. Using thermal activation measurements we are able to distinguish between contributions to H_{ex} arising from the thermal stability of the antiferromagnetic particles (bulk behaviour) and that due to changing interface density with increasing Co concentration. We have interpreted our results in terms of the independent particle volume model.

Keywords: Exchange Bias, Magnetic Nanocomposites.

1. INTRODUCTION

The phenomenon of exchange bias is the shift of the magnetization hysteresis loop along the field axis and occurs due to interfacial coupling of ferromagnetic (FM) and antiferromagnetic (AFM) spins. Although initially discovered on naturally oxidized Co nanoparticles,¹ it has been studied most widely in polycrystalline FM/AFM bilayers. Recently these studies have been extended to various systems of FM nanoparticles embedded in AFM matrices, e.g., Co–Mn,² Co–CoO,³ Fe–Cr₂O₃⁴ etc. The theoretical understanding of such composite FM/AFM systems is far more complex than that of FM/AFM bilayers. The exchange bias effect is known to depend upon the thicknesses of the FM and AFM layers in bilayer systems. This raises the question of how a ‘thickness’ can be defined in a FM/AFM composite material. As a first approximation, the diameter of the FM particles is considered to be analogous to the FM layer thickness, while the interparticle distance is taken to be analogous to the AFM thickness.⁵ These quantities depend on the FM to AFM ratio and/or the particle size in a given composite system.

Although several models exist for the explanation of exchange bias in FM/AFM bilayers, efforts to theoretically model the behavior of nanocomposites have been limited, mainly due to the complex morphology of these systems.

* Author to whom correspondence should be addressed.

Delivered by Ingenta to:
Institute of Molecular and Cell Biology

IP: 137.132.203.60

Thu, 01 Sep 2011 08:26:44

Also, most models invoke the Heisenberg direct exchange interaction, which cannot be used to describe superexchange coupled oxide AFM's. A recently proposed model⁶ takes into account the interfaces, relative molar volumes of the FM and AFM and a mean field term due to dipolar interactions. The exchange bias obtained is inversely proportional to the FM particle radius r . The samples investigated in Ref. [6] had the same average particle size in the FM and AFM, but this is generally not the case specially for metal/metal oxide systems.^{4–5}

In this paper we show that the particle size and size distribution in the AFM play an important role in determining the magnitude and concentration dependence of H_{ex} . The concentration of the FM part was varied while the particle sizes in the FM were kept similar in all samples. The same was done for the AFM particles in order to distinguish between the particle density and particle size dependent effects and the role of the FM/AFM interfaces on H_{ex} . We show that exchange bias in these complex systems can be explained using the *independent AFM particle volume model*, which we have previously successfully applied to FM/AFM thin films.⁷ According to this model, the magnitude of the exchange bias depends upon the degree of order in the AFM, which is determined by thermal activation over grain volume dependent energy barriers, moderated by an interfacial coupling constant C^* .^{7–9} The order in the AFM is established during the setting process which

involves cooling the AFM from above its Néel temperature T_N in the presence of the exchange field from the FM. The exchange bias is then given by:

$$H_{\text{ex}} = C^* H_{\text{ex}}^i \int f(V) dV \quad (1)$$

Here H_{ex}^i is the intrinsic value of the exchange bias provided that the FM/AFM interface is perfectly flat. C^* is an interfacial coupling constant which takes into account the degree of disorder at the FM/AFM interface. $f(V)$ is the volume distribution of the AFM particles, which in fine particle systems is known to be a log-normal function.¹⁰ Using $V = V/V_m$, where V_m is the median particle volume and σ the standard deviation, the log-normal distribution is given by:

$$f(y) = \frac{1}{\sigma y \sqrt{2\pi}} \exp\left(-\frac{(\ln y)^2}{2\sigma^2}\right) \quad (2)$$

2. EXPERIMENTAL DETAILS

Co–Cr₂O₃ samples were prepared using the sol gel technique.¹¹ The following sample batches were prepared: A (30 wt% Co), B (40 wt% Co), C (50 wt% Co), C1 (50 wt% Co), D (60 wt% Co) and E (80 wt% Co). These compositions were confirmed by EDX. Samples in each series were annealed at 500 °C for 2 hrs. to obtain different sizes of the Co and Cr₂O₃ particles. Sample C1 was obtained by annealing sample C twice. Magnetic measurements were done on a Lakeshore 4500 VSM fitted with a continuous flow He cryostat.

3. RESULTS AND DISCUSSION

XRD analysis showed that all samples consist of rhombohedral Cr₂O₃ and fcc Co. Samples A, B, C, D and E have the same average particle size of ~24 nm and sample C1 has a size of 34 nm in the AFM. This can be also be seen in the TEM images shown in Figure 1, which clearly show cobalt nanoparticles of average diameter $D_{\text{Co}} \approx 3.5$ nm embedded in a matrix of Cr₂O₃ nanoparticles.

For thermal activation measurements each sample was heated in a positive applied field to a setting temperature

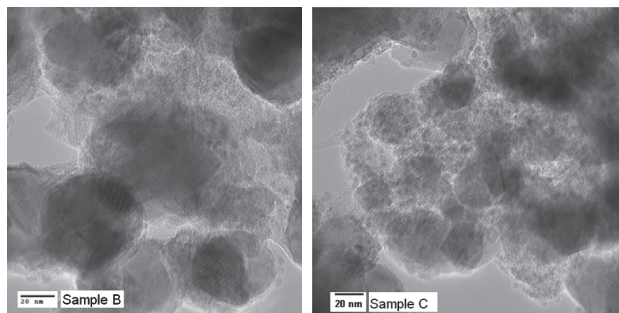


Fig. 1. TEM images of Co–Cr₂O₃ nanocomposite samples B and C.

$T_{\text{SET}} > T_N$. It was then cooled to a temperature T_{NA} , at which the AFM is free from thermal activation effects. The field was then reversed and the sample was heated for 30 mins. at an activation temperature T_{ACT} causing part of the AFM particle volume distribution to align opposite to the original setting direction. T_{ACT} corresponds to a critical AFM particle volume V_C that can be thermally reversed against the original setting direction.⁹ So only AFM particles with $V > V_C$ will contribute to H_{ex} . Because thermal activation is used to set or activate the AFM, the corresponding particle volumes can be written as $V_{\text{SET}, C} = \ln(\tau f_o) k_B T / K_{\text{AF}}(T)$, where τ is the setting time in case of V_{SET} and the activation time in case of V_C and T is the corresponding setting or activation temperature.⁷ The sample is then cooled down to T_{NA} and the $M(H)$ loop is measured. A detailed description of this measurement procedure is given in Ref. [7]. Figure 2 shows the results of these measurements. The solid lines represent values of the integral $\int_{V_C}^{V_{\text{SET}}} f(V) dV$, where $f(V)$ is obtained from Eq. (2). In our model, I represents the fraction of the AFM particles that are contributing to H_{ex} after activation at a given temperature. Figure 2 shows good correspondence between the behaviour of H_{ex} and I . This means that the measured values of H_{ex} are largely controlled by thermal activation effects over AFM particle volume dependent energy barriers as described by the integral I . There is good agreement between H_{ex} and I for sample A and this becomes poorer as the FM particle concentration and the FM/AFM interface density increases. At higher FM/AFM interface densities, the thermally activated depinning of interfacial spins which affects the coupling constant C^* may be responsible for the weaker agreement between H_{ex} and I for higher Co concentrations. This is more pronounced at lower values of T_{ACT} because smaller AFM particles are expected to have a larger proportion of loosely coupled surface spins. Thermally activated depinning of these surface spins would result in smaller values of H_{ex} .

Applying the independent AFM particle volume model requires prior knowledge of the AFM particle size distribution $f(V)$. For AFM thin films, $f(V)$ is obtained through particle size analysis of TEM images. This analysis becomes very difficult and less accurate for FM/AFM nanocomposites because of poor TEM contrast of oxide AFM's and the composite nature of the samples. To circumvent this problem, the integral I was calculated from Eq. (1) with $f(V)$ obtained from Eq. (2) and using σ as a floating parameter. σ was found to lie in the range 0.17..0.18 for samples A, B and C, and $\sigma = 0.22$ for sample C1. The temperature at which $H_{\text{ex}} = 0$ corresponds to the median blocking temperature T_b of the sample.⁷ Assuming spherical particles, D_m can be calculated from T_b using⁷

$$D_m = \left(\frac{6 \ln(\tau f_o) k_B < T_b >}{\pi K_{\text{AF}}(< T_b >)} \right)^{1/3} \quad (3)$$

Here $\tau = 1800$ s is the thermal activation time, $f_o \sim 10^9$ s⁻¹ is an attempt frequency, k_B is the Boltzmann constant and

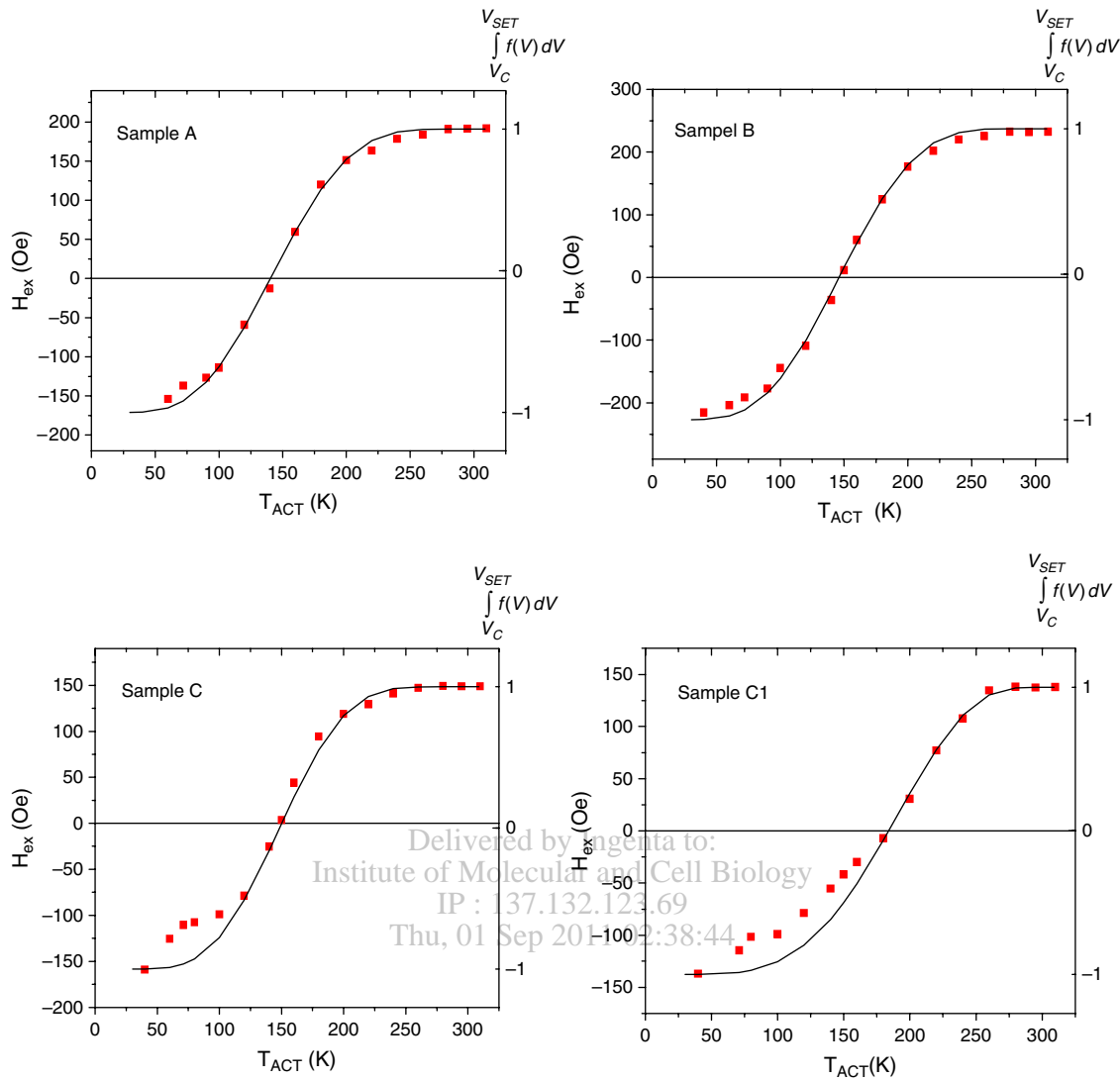


Fig. 2. Thermal activation measurement of samples A, B, C and C1. Solid lines are calculated values of the integral shown on the right axis.

K_{AF} the anisotropy constant of Cr₂O₃ · $K_{AF}(T_b)$ was calculated using,

$$K_{AF}(T) = K_{AF}(0) \left(1 - \frac{T}{T_N} \right) \quad (4)$$

where $K_{AF}(0) = 2 \times 10^5 \text{ erg cm}^{-3}$ and $T_N = 308 \text{ K}$.¹² Using values of T_b obtained from Figure 2, the median AFM particle diameters for all samples have been calculated from Eq. (3), giving $D_{Cr_2O_3}$ of about 26 nm for samples A, B and C and 34 nm for sample C1. These values agree well with those obtained from analysis of the XRD spectra. Figure 2 shows that T_b depends only upon the average particle size $D_{Cr_2O_3}$ in the AFM and is independent of the FM content of our samples. Samples A, B and C, having the similar values of $D_{Cr_2O_3}$, have $T_b \sim 148 \text{ K}$, while sample C1 has a $T_b = 185 \text{ K}$.

These results show that the AFM particles are *non-interacting, and not coupled into domains*, because changing the concentration would affect the correlation length

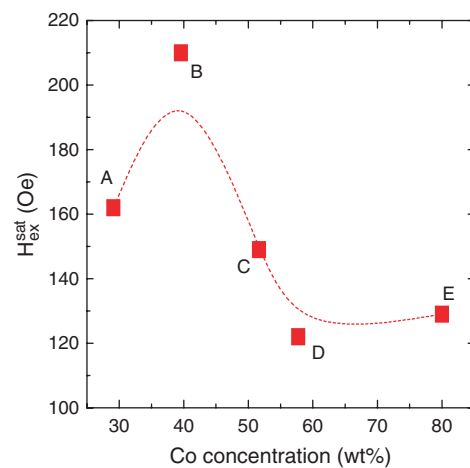


Fig. 3. H_{ex}^{sat} measured at 77 K after activation at $T_{ACT} = 310 \text{ K}$. Dashed line is guide to the eye.

and T_b . This in turn means that the superexchange interaction is not transmitted across the particle boundaries. Superexchange between the Cr³⁺ cations is mediated by O²⁻ anions and is very sensitive to the bond lengths and bond angles between them. Symmetry breaking and disorder at the surface of the nanoparticles would lead to a strong disruption of the superexchange interaction, effectively decoupling the Cr₂O₃ particles.

An interesting aspect of working with Cr₂O₃ is that it can be field cooled from a paramagnetic state above T_N . This allows the *entire* particle volume distribution to be set. If measurements are made at T_{NA} , where there is no thermal activation, the integral in Eq. 1 becomes unity. The saturation value of exchange bias, H_{ex}^{sat} , measured at high activation temperature $T_{ACT} = 310$ K then corresponds to $C^*H_{ex}^i$ enabling us to isolate that part of H_{ex} that depends upon the FM/AFM interface density. This had not been possible in our earlier work on NiFe/FeMn and CoFe/IrMn thin films because of the high T_N of metallic AFM's. Figure 3 shows H_{ex}^{sat} versus Co concentration for the five samples studied. It has a maximum at 40 wt% after which it decreases due to percolation effects. Because the AFM is completely set at $T_{ACT} = 310$ K, the behaviour shown in Figure 3 is only due to changing FM/AFM interface density. At all lower activation temperatures a *mixture of bulk and interfacial effects* influence the value of H_{ex} .

4. CONCLUSIONS

The exchange bias in Co–Cr₂O₃ nanocomposites can be explained using the independent particle volume model. The median blocking temperature depends only upon the median particle volume in the AFM. This implies that the

AFM particles act independently and are not coupled into domains, indicating that superexchange does not transmit across particle boundaries. Our measurement technique allows us to isolate the parameter $C^*H_{ex}^i$ which is a measure of the intrinsic exchange bias moderated by interfacial effects.

Acknowledgments: Sadia Manzoor and M. Farooq Nasir are grateful for financial support from the CIIT and the HEC, Government of Pakistan (Grant # 261 and PIN # 063-112020-Ps3-115). We also thank Dr. U. Manzoor for help with the TEM images.

References and Notes

1. W. H. Meiklejohn and C. P. Bean, *Phys. Rev.* 102 1413 (1956).
2. N. Domingo, D. Fiorani, A. M. Testa, C. Binns, S. Baker, and J. Tejada, *J. Phys. D: Appl. Phys.* 41, 134009 (2008).
3. J. A. De Toro, J. P. Andrés, J. A. González, P. Muñoz, T. Muñoz, P. S. Normile, and J. M. Riveiro, *Phys. Rev. B* 73, 094449 (2006).
4. J. Sort, V. Langlais, S. Doppiu, B. Dieny, S. Suriñach, J. S. Muñoz, M. D. Baño, Ch. Laurent, and J. Nogués, *Nanotechnology* 15, S211 (2004).
5. J. Nogués, J. Sort, V. Langlais, S. Doppiu, B. Dieny, J. S. Muñoz, S. Suriñach, M. D. Baro, S. Stoyanov, and Y. Zhang, *Int. J. Nanotechnology* 2, 23 (2005).
6. D. R. Cornejo, E. Padrón Hernández, A. Azevedo, and S. M. Rezende, *J. Appl. Phys.* 97, 10K103 (2005).
7. L. E. Fernández-Outón, G. Vallejo-Fernández, Sadia Manzoor, B. Hillebrands, and K. O'Grady, *J. Appl. Phys.* 104, 093907 (2008).
8. L. E. Fernández-Outón, G. Vallejo-Fernández, and K. O'Grady, *J. Appl. Phys.* 103, 07C106-1 (2008).
9. L. E. Fernández-Outón, K. O'Grady, and M. J. Carey, *J. Appl. Phys.* 95, 6853 (2004).
10. C. G. Granqvist and R. A. Buhrman, *J. Appl. Phys.* 47, 2200 (1976).
11. P. A. Kumar and K. Mandal, *J. Appl. Phys.* 101, 113906 (2007).
12. S. Foner, *Phys. Rev.* 130, 183 (1963).

Received: 16 June 2009. Accepted: 21 October 2009.